

Hadronic uncertainties of inclusive atmospheric lepton fluxes from fixed-target experiments

Anatoli Fedynitch^{a,*} and Matthias Huber^b

^a*Institute for Cosmic Ray Research, The University of Tokyo,
5-1-5 Kashiwa-no-ha, 277-8582 Kashiwa, Chiba, Japan*

^b*Technische Universität München, Physik-Department,
James-Frank-Str.1, D-85748 Garching bei München, Germany*

E-mail: afedyni@icrr.u-tokyo.ac.jp

Theoretical atmospheric neutrino flux estimates serve as a crucial input for the determination of the neutrino mass hierarchy, the unitarity of the PMNS matrix and the atmospheric mixing angle θ_{23} in underground neutrino detectors, such as the Super-Kamiokande, IceCube DeepCore and KM3Net ORCA. With the expected reduction of detector-induced systematic uncertainties by the IceCube Upgrade, and the substantial gain in effective volume of the upcoming Hyper-Kamiokande and KM3NeT ORCA detectors, the theoretical uncertainty of the non-oscillated neutrino flux and flavor composition will ultimately impact the achievable precision of future measurements. In this work, we tackle the uncertainty associated with modeling of hadronic interactions, which has the largest effect on the calculation. We develop an empirical, data-driven model (DDM), derived from high-precision accelerator data from the recent CERN North Area (NA) fixed-target experiments, and a few simple model-dependent arguments. The model is well constrained in the intermediate energy range above a few GeV up to a hundred GeV and achieves good agreement with atmospheric muon data without explicitly using it. We compare our result to reference calculations of the atmospheric neutrino flux.

*37th International Cosmic Ray Conference (ICRC 2021)
July 12th – 23rd, 2021
Online – Berlin, Germany*

*Presenter

Experiment	beam	$E_{\text{beam}}/\text{GeV}$	Secondaries	Variables
NA49	pC	158	π^\pm, p, n	x_F, p_\perp
NA49	pp	158	K^\pm	x_F, p_\perp
NA61/SHINE	pC	31	$\pi^\pm, K^\pm, K_S^0, \Lambda$	p, θ
NA61/SHINE	π^-C	158, 350	$\pi^\pm, K^\pm, p, \bar{p}$	p, p_\perp

Table 1: Summary of particle yield measurements from NA49 [5, 6] and NA61/SHINE [4, 7]. DDM is built using the double-differential yields in the variables indicated in the last column.

1. Introduction

The interactions of cosmic rays with the Earth’s atmosphere create cascades of stable and unstable particles some of which decay into atmospheric leptons [1, 2]. These atmospheric muons and neutrinos are of particular interest since they serve as natural “beam” for deep underground large volume detectors such as the Super-/Hyper-Kamiokande, the IceCube Observatory with its low-energy extension DeepCore and its Upgrade, and the ORCA low-energy array of the KM3NeT. For the growing volumes of low-background Dark Matter experiments and those looking for exotic particles or the Diffuse Supernova background, atmospheric neutrinos constitute irreducible background.

Conventional calculations of atmospheric lepton fluxes start from the spectrum and composition of cosmic rays, track secondary particle cascades down to the ground, and in case of neutrinos take into account the flavor oscillations that occur on their way through the atmosphere and the planet. The common calculation methods are semi-analytical solutions of cascade equations, full Monte Carlo calculations (tracking each particle cascade particle individually), and iterative numerical solutions, *e.g.* with MCEQ [3].

In this work, we adapt a data-driven empirical model for the parameterization of secondary particle production, eliminating the impact of a phenomenological microscopic model for particle interactions typically implemented as Monte Carlo event generators. Our method significantly reduces the model-dependence in the uncertainty estimation, and produces a data-driven atmospheric lepton flux prediction with a few controllable extrapolations.

1.1 Parametrization of data and its uncertainties

The Data Driven Model (DDM) is exclusively based on the sets in Tab. 1, taken with thin carbon targets. As pointed out in [8], the absence of a charged kaon analysis for proton-carbon at 158 GeV in NA49 and NA61/SHINE is essential and requires a workaround. We use charged kaon data from pp collisions at NA49 [6] and extrapolate the data to proton-carbon using a combination of interaction models. The NA49 data is provided in the center of mass frame variable $x_F \approx p_z/\sqrt{s}$ and requires a transformation into target rest frame. This is done by fitting p_\perp distribution in each x_F bin and a bootstrap method to convert from the $x_F - p_\perp$ to $x_{\text{Lab}} - p_\perp$. The single-differential x_{Lab} distribution is obtained by integrating over p_\perp . The experimental error, approximated as the geometrical sum of statistical and systematic error, is also propagated throughout this process. The NA61 data is published as a function of scattering angle and total laboratory momentum $\theta - p$, hence single-differential distributions can be readily obtained through integration over θ .

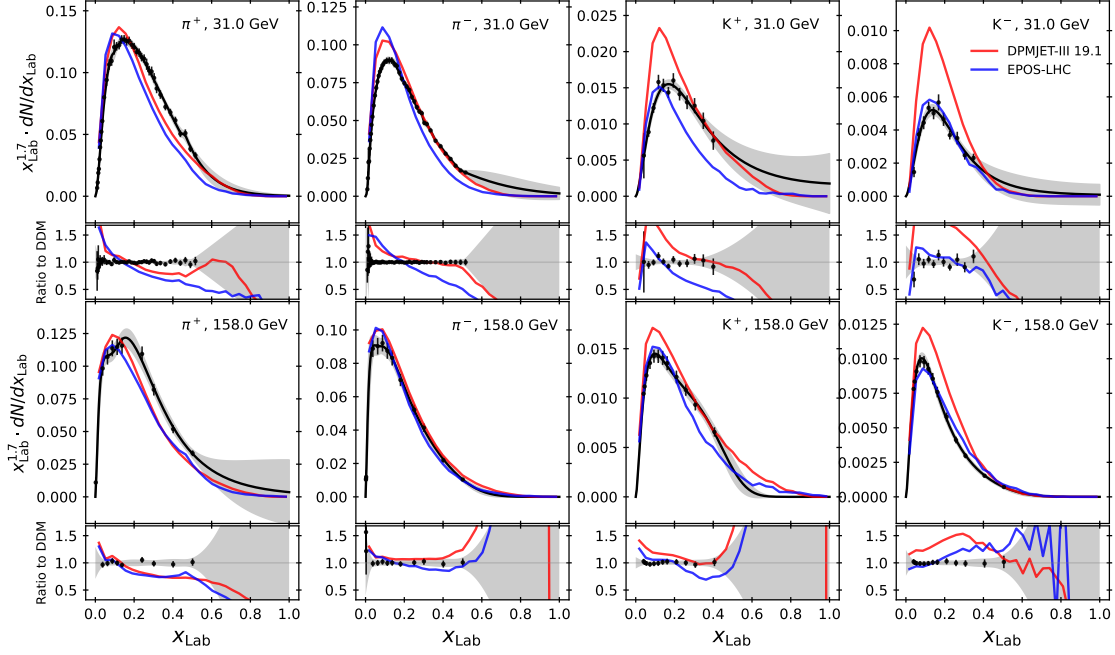


Figure 1: Parametrization of light meson yields. The data points in the upper panels are for proton-carbon collisions at 31 GeV from NA61/SHINE [4], integrated over scattering angle. The lower panels show NA49 proton-carbon data at 158 GeV, transformed into laboratory frame and integrated over p_{\perp} [5]. The data points for K^{\pm} are extrapolated to proton-carbon from NA49 proton-proton data [6]. Black curves represent the DDM spline fits with corresponding error band. Reference hadronic interaction models are shown in color and appear larger as in usual comparisons due to the linear scale, and the factor $x_{\text{Lab}}^{1.7}$ that helps to emphasize the relevant phase space for the Z-factor integrals in .

The natural logarithm of the data has been used to fit cubic splines to the meson yields in Fig. 1. The exception are the π^{\pm} data at 31 GeV, which require linear splines for robust fits. A smoothing factor $s > 0$ has been chosen such that the fit follows all trends in the data, and the error on the Z-factor stabilizes for larger values of s . The spline uncertainties, derived by computing a Hesse matrix via finite differences, have been increased by factor two that improves the containment of the 1σ error bars by the uncertainty band. By comparing the ratio panels in Fig. 1 with each other, it can be seen that the errors increase similarly in the absence of data. The uncertainty is, therefore, largely driven by the position of the right most data point.

1.2 Hadronic model assumptions

Fig. 2 shows the energy-dependent spectrum-weighted moments computed from the data in Tab. 1 and from current hadronic interaction models. The Z-factors (see, *e.g.* [2, 10])

$$Z_{Nh}(E_N) = \int_0^1 dx_{\text{Lab}} x_{\text{Lab}}^{\gamma(E_N)-1} \frac{dN_{N \rightarrow h}}{dx_{\text{Lab}}}(E_N). \quad (1)$$

are a sufficient framework to discuss extrapolation uncertainties. A consistent interaction model is constructed starting from an initial library of particle yields from DPMJET and then replacing

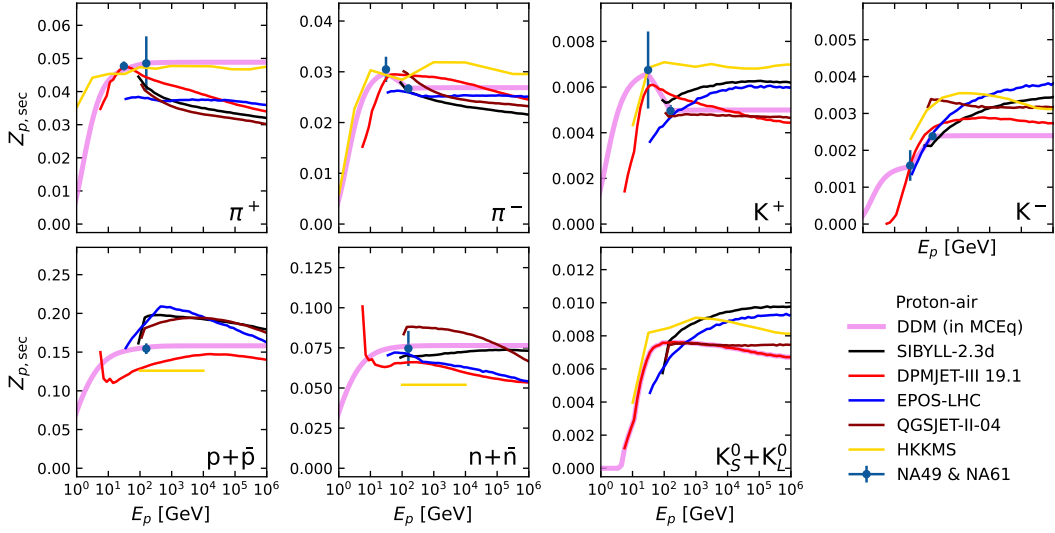


Figure 2: Energy-dependent spectrum-weighted moments (Z -factors) computed for an air target and $\gamma = 2.7$ according to Eq. 1. The result of the HKKMS interaction model, which is based on an older version of DPMJET-III and has been tuned inclusive muons [9], is shown in gold. Strict Feynman-scaling, recognizable as approximate energy independence, is not favored by most of the models. In DDM, scaling appears by construction above 158 GeV (see text). In HKKMS, scaling is a result of tuning their calculation to inclusive muon observations.

the yields by that known to DDM. The strongest assumption in DDM is Feynman scaling (FS) [11]. In simplified terms, the idea is that once partons scatter and form color-chains (or -strings), there is a universal minimal cost to pull new partons from the vacuum once a critical string tension is exceeded. At higher collision energies, the longitudinal phase-space grows but the number of secondaries per phase-space element is constant. As a consequence, the longitudinal momentum spectrum in the scaling variable x_F is independent of energy. Although this is a very simplified view on the complexity of hadron scattering, the idea catches some essentials of non-perturbative modeling of interactions and is approximately realized in data. Within a limited p_\perp range, LHCf demonstrated that FS holds at LHC energies [12]. FS is known to be violated due to the significant contribution of hard processes at central rapidities and high energies, due to multiple partonic interactions. Some violation of forward scaling is also expected due to, *e.g.*, the energy-dependence of diffractive cross sections and significant contributions of resonances to the inclusive yields of light hadrons [6, 8, 13].

Nonetheless, we assume FS for DDM above 158 GeV for three reasons: 1. The violation known for central or hard scatterings is suppressed for inclusive fluxes due to the factor $x_{\text{Lab}}^\gamma - 1$ in Eq. (1); 2. There is no clear, consistent trend in data in more complicated models; 3. Any other assumption, or an attribution of some error, is a stronger source of bias to the data-driven approach. Since only two suitable datasets are included, DDM interpolates between the 31 GeV and 158 GeV data linearly in $\log(E_p)$. Once new data are released by NA61, these will be included to allow for a more sophisticated transition and serve as additional cross check. At energies lower than 31 GeV "FS" is applied again, however due to the shrinking phase-space the distributions in Fig. 2 tend to zero.

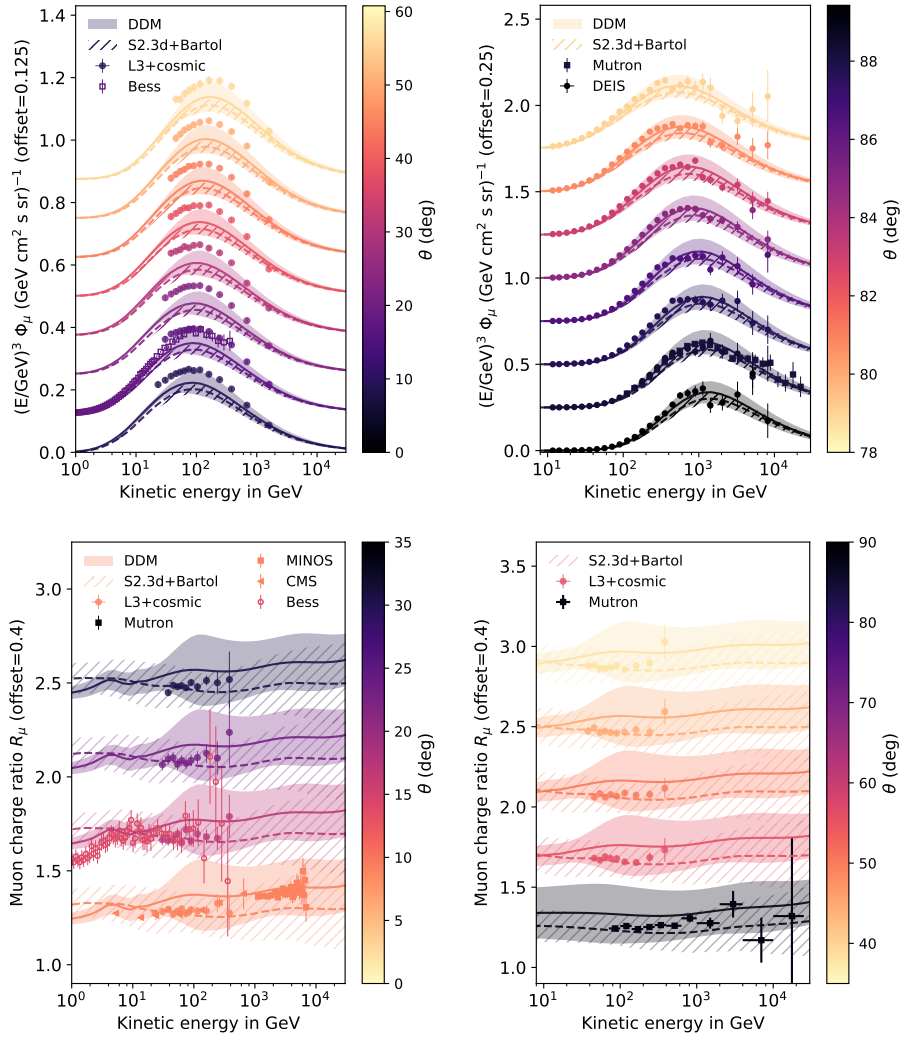


Figure 3: Near-vertical (left panels) and near-horizontal (right panels) muon flux and muon charge ratio, compared with various experiments [14–19], and our previous calculation based on SIBYLL and *Bartol* errors [10, 20, 21]

Additional model assumptions are isospin symmetry for leading particles, see *e.g.* [2], and the production (inelastic) interaction cross sections are that from DPMJET-III 19.1. Using carbon instead of air target was found to be negligible ($< 1\%$). Additional, minor simplifications originate from MCEQ as cascade code, such as superposition primary projectile nuclei.

2. Comparison with atmospheric lepton data

Comparisons with atmospheric muon measurements by spectrometers at the surface are shown in Fig. 3. The data is subject to larger shifts due to systematic uncertainties which are not shown for most of it. The new and the previous model lack vertical intensity but fit well to near-horizontal measurements. This “tension” is weaker for the DDM model since the errors are larger, dominated

by π^+ at higher energies. Whether this apparent tension is real, is beyond the scope of this contribution, however one may speculate that this points to a) that the Feynman scaling assumption does not hold, or b) the complicated shape of cosmic ray flux and its neutron fraction is not well represented by the central value of the Global Spline Fit [22]. In the more likely, latter case, the nucleon spectrum would have to shift up at TeV energies by a few percent and then soften at higher energies within the error bands of the Global Spline Fit [22]. Since the uncertainties on the muon data are much smaller than that of DDM, we can expect to successfully calibrate the model using these data (see contribution by J.P. Yáñez [23]).

The neutrino fluxes in the top panels Fig. 4 are compatible with our previous calculations using SIBYLL and *Bartol* errors above a few GeV. For ν_e fluxes, the agreement with Super-K data below a few GeV is excellent, while in ν_μ this is not really the case, although both originate from muon decay at this energies. Note that none of the model predictions is corrected for disappearance seen in the ν_μ flux data. Prompt fluxes are not included in DDM since there is insufficient data to perform a data-driven parametrization. Uncertainties from cosmic ray fluxes are not shown, which would mainly impact higher energies above the TeV range. The neutrino ratios in the lower panels of Fig. 4 profit most significantly from the new uncertainties. Both neutrino/anti-neutrino ratios are compatible with previous calculations including that by HKKMS within errors and over wide ranges in energy. The error estimates notably shrunk at high and low energies due to the smaller uncertainty on low energy mesons and high energy kaons. However, for the flavor ratio in the bottom panel both, the SIBYLL and the DDM calculation, have more ν_μ , largely driven by smaller kaon production.

3. Conclusion and outlook

This new Data-Driven Model (DDM) attacks the largest source of uncertainty in atmospheric neutrino flux calculations. Data from fixed-target accelerators and its uncertainties have been successfully parameterized with splines. The resulting errors on the lepton fluxes and ratios considerably shrink at low energies and high energies, staying compatible at tens – hundreds GeV with the previous reference calculations. The main sources of the remaining uncertainty are π^+ at somewhat larger x_{Lab} and charged kaon measurements on carbon target and at higher energy. The change in the flavor ratio may impact atmospheric neutrino oscillation analyses.

In very near future, NA61 aims to publish more data between 10 – 158 GeV. Depending on the precision, we may be able to push neutrino flux errors down to 3-5%. At higher energy, data from NA59 taken on beryllium target may add crucial pieces of information if it remains precise after extrapolation from Be→C. As alternative cross check and further sources of constraints from data, DDM can be calibrated using inclusive muon measurements from surface spectrometers [23, 29]. At high energies, we aim to use deep underground muon intensity data that are suitable to verify the model and reduce high energy uncertainties [30]. The characterization of primary cosmic ray flux uncertainties will become crucial to obtain the best model.

Acknowledgements A.F. performed this work as JSPS International Research Fellow (JSPS KAKENHI Grant Number 19F19750) and acknowledges the support by the Institute for Cosmic Ray Research, The University of Tokyo.

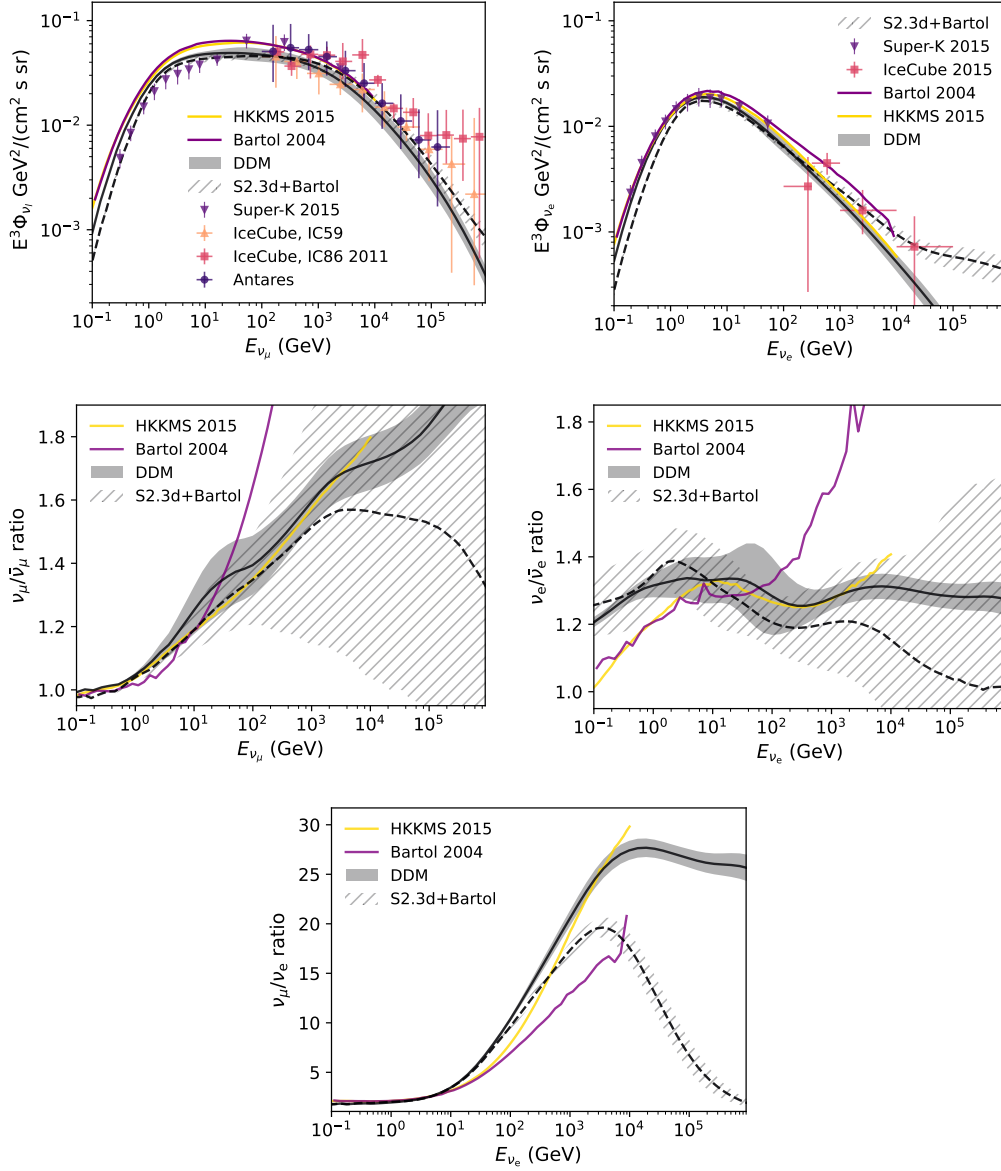


Figure 4: Zenith-averaged atmospheric neutrino fluxes and ratios: top left $\nu_\mu + \bar{\nu}_\mu$ and right $\nu_e + \bar{\nu}_e$; center left $\nu_\mu/\bar{\nu}_\mu$ and right $\nu_e/\bar{\nu}_e$; and bottom $(\nu_\mu + \bar{\nu}_\mu)/(\nu_e + \bar{\nu}_e)$. Data are from IceCube, Antares and Super-K [24–28].

References

- [1] T. K. Gaisser and M. Honda, *Ann. Rev. Nucl. Part. Sci.* **52** (2002) 153–199.
- [2] T. K. Gaisser, R. Engel, and E. Resconi, *Cosmic Rays and Particle Physics*. Cambridge University Press, 2016.
- [3] A. Fedynitch et al., *EPJ Web of Conferences* **99** (2015) 08001.
- [4] NA61/SHINE Collaboration, N. Abgrall et al., *Eur. Phys. J. C* **76** (2016) 84.

- [5] **NA49** Collaboration, C. Alt et al., *Eur. Phys. J. C* **49** (2007) 897–917.
- [6] **NA49** Collaboration, T. Anticic et al., *Eur. Phys. J. C* **68** (2010) 1–73.
- [7] **NA61/SHINE** Collaboration, R. R. Prado, *EPJ Web Conf.* **208** (2019) 05006.
- [8] A. Fedynitch, F. Riehn, R. Engel, T. K. Gaisser, and T. Stanev, *Phys. Rev. D* **100** (2019) 103018.
- [9] T. Sanuki, M. Honda, T. Kajita, K. Kasahara, and S. Midorikawa, *Phys. Rev. D* **75** (2007) 043005.
- [10] **IceCube** Collaboration, A. Fedynitch and J.-P. Yáñez, PoS(ICRC2019)882 (2020).
- [11] R. P. Feynman, *Phys. Rev. Lett.* **23** (1969) 1415–1417. [,494(1969)].
- [12] **LHCf** Collaboration, O. Adriani et al., *Phys. Rev. D* **94** (2016) 032007.
- [13] F. Riehn, R. Engel, A. Fedynitch, T. K. Gaisser, and T. Stanev, *Phys. Rev. D* **102** (2020) 063002.
- [14] **L3** Collaboration, P. Achard et al., *Phys. Lett. B* **598** (2004) 15–32.
- [15] O. C. Allkofer, H. Jokisch, G. Klemke, Y. Oren, R. Uhr, G. Bella, and W. D. Dau, *Nucl. Phys. B* **259** (1985) 1–18. [Erratum: Nucl. Phys.B268,747(1986)].
- [16] S. Haino et al., *Phys. Lett. B* **594** (2004) 35–46.
- [17] **CMS** Collaboration, V. Khachatryan et al., *Phys. Lett. B* **692** (2010) 83–104.
- [18] **OPERA** Collaboration, N. Agafonova et al., *Eur. Phys. J. C* **74** (2014) 2933.
- [19] S. Matsuno et al., *Phys. Rev. D* **29** (1984) 1–23.
- [20] G. D. Barr, T. K. Gaisser, S. Robbins, and T. Stanev, *Phys. Rev. D* **74** (2006) 094009.
- [21] A. Fedynitch, H. P. Dembinski, R. Engel, T. K. Gaisser, F. Riehn, and T. Stanev, PoS(ICRC2017)301 (2017).
- [22] H. P. Dembinski, R. Engel, A. Fedynitch, T. Gaisser, F. Riehn, and T. Stanev, PoS(ICRC2017)533 (2018). [35,533(2017)].
- [23] J.-P. Yáñez and A. Fedynitch, PoS(ICRC2021)1149 (2021).
- [24] **Super-Kamiokande** Collaboration, E. Richard et al., *Phys. Rev. D* **94** (2016) 052001.
- [25] **IceCube** Collaboration, M. Aartsen et al., *Eur. Phys. J. C* **75** (2015) 116.
- [26] **IceCube** Collaboration, P. Heix, S. Tilav, C. Wiebusch, and M. Zöcklein, PoS(ICRC2019)465 (2020).
- [27] **ANTARES** Collaboration, S. Adrian-Martinez et al., *Eur. Phys. J. C* **73** (2013) 2606.
- [28] **IceCube** Collaboration, M. G. Aartsen et al., *Phys. Rev. D* **91** (2015) 122004.
- [29] J.-P. Yáñez, A. Fedynitch, and T. Montgomery, PoS(ICRC2019)881 (2019).
- [30] W. Woodely, A. Fedynitch, and M.-C. Piro, PoS(ICRC2021)1226 (2021).